Research Square

Preprints are preliminary reports that have not undergone peer review.
They should not be considered conclusive, used to inform clinical practice,
or referenced by the media as validated information.

Computational Study of Natural Photosensitizers for Dye-Sensitized Solar Cells: DFT and TD-DFT Approach

Shahriar Siam
University of Rajshahi
Apel Mahamud Rabby
University of Rajshahi
Jewel Hossen
jewelhossenruet@gmail.com
Rajshahi University of Engineering & Technology
Tanu Dey
University of Rajshahi
Md. Tanvir Rashid Rezvi
University of Rajshahi
Md. Al-Amin-Al-Azadul Islam
Rajshahi University of Engineering & Technology
Shafikul Islam
Jahangirnagar University

Research Article

Keywords: Natural photosensitizers, DSSC, DFT, TD-DFT, Photovoltaic properties

Posted Date: November 20th, 2026

DOI: https://doi.org/10.21203/rs.3.rs-11697388/v1

License: This work is licensed under a Creative Commons Attribution 4.0 International License.
Read Full License

Additional Declarations: No competing interests reported.

Computational Study of Natural Photosensitizers for Dye-Sensitized Solar Cells: DFT and TD-DFT Approach

Shahriar Siam[1], Apel Mahamud Rabby[1], Jewel Hossen[2,*], Tanu Dey[1], Md. Tanvir Rashid Rezvi[1], Md. Al-Amin-Al-Azadul Islam[2], Shafikul Islam[3]

[1]Department of Applied Chemistry and Chemical Engineering, University of Rajshahi, Rajshahi-6205, Bangladesh. Email: shahriarsiam978@gmail.com, apelmahamudrabby947@gmail.com, tanudey4002@gmail.com, tanvirrashid267@gmail.com

[2]Department of Chemistry, Rajshahi University of Engineering & Technology, Rajshahi-6204, Bangladesh. Email: mailto:jhossen@chem.ruet.ac.bd, aamin@chem.ruet.ac.bd

[3]Department of Chemistry, Jahangirnagar University, Savar, Dhaka-1342, Bangladesh. Email: chem.shafik@juniv.edu

*Corresponding author: Dr. Jewel Hossen, Email: jewelhossenruet@gmail.com, jhssen@chem.ruet.ac.bd

Abstract

Natural photosensitizers offer promising alternatives for sustainable dye-sensitized solar cells (DSSCs). This study systematically investigates the electronic, optical, and photovoltaic properties of four natural pigments acetylshikonin (ASK), shikonin (SKN), pseudodeoxyviolacein (PDV), and violacein (VLC) using density functional theory (DFT) and time-dependent DFT (TD-DFT). Calculations were performed at the B3LYP/6-311G(d,p) and CAM-B3LYP/6-311G(d,p) levels to evaluate electronic structures, absorption characteristics, and photovoltaic descriptors in the gas phase and acetonitrile. PDV exhibited the narrowest HOMO–LUMO gaps (1.791–1.980 eV) and longest absorption wavelengths (735.71–767.02 nm), indicating favourable near-infrared light harvesting. Conversely, VLC demonstrated the highest oscillator strengths (0.6071–0.7115) and light-harvesting efficiencies (0.753–0.806), together with the strongest electron injection driving forces (−1.544 to −1.267 eV). PDV also exhibited the longest estimated radiative lifetime (49.808–51.006 ns). Meanwhile, ASK and SKN showed more favourable dye regeneration energetics and higher theoretical voltage-related descriptors. The pigments exhibited thermodynamically feasible electron injection and regeneration within the adopted model. Overall, VLC and PDV emerged as promising DSSC sensitizers with complementary optical and charge-transfer advantages, providing a theoretical foundation for further molecular optimization and experimental validation.

Keywords: Natural photosensitizers; DSSC; DFT; TD-DFT; Photovoltaic properties.

1. Introduction

The growing demand for sustainable and efficient solar-energy technologies has stimulated continued interest in dye-sensitized solar cells (DSSCs) [1, 2]. Since the pioneering demonstration of TiO_2-based DSSCs, these devices have attracted considerable attention because light absorption and charge transport are spatially separated, allowing the sensitizer to be molecularly engineered for efficient photon harvesting [3, 4]. In a typical DSSC, the dye absorbs solar radiation, undergoes photoexcitation, and injects an electron into the conduction band (CB) of TiO_2. The oxidized dye is subsequently regenerated by a redox mediator [5–7]. Accordingly, the electronic structure of the sensitizer plays a central role in determining the energetics of photoinduced electron injection, dye regeneration, and light harvesting [8].

An efficient DSSC sensitizer should therefore exhibit strong and broad absorption in the solar spectrum together with suitable frontier orbital energies and favourable excited-state energetics. In particular, the excited-state energy must provide sufficient driving force for electron injection into the TiO_2 conduction band, while the oxidized dye must remain energetically accessible for regeneration by the redox couple [5, 9]. The spatial distribution of the frontier molecular orbitals, excitation energy, oscillator strength, and excited-state lifetime can further influence the likelihood of productive charge-transfer processes. Consequently, evaluating these parameters collectively is essential for identifying promising sensitizers rather than relying solely on their absorption maxima.

Natural pigments have emerged as attractive alternatives to conventional synthetic sensitizers because of their structural diversity, renewable origin, and potentially lower environmental and economic burden [10, 11]. Numerous natural compounds, including anthocyanins, chlorophylls, carotenoids, betalains, and flavonoids, have been investigated for DSSC applications [12–15]. However, their photovoltaic potential is frequently limited by insufficient spectral coverage, unfavourable energy-level alignment, weak semiconductor interaction, excited-state deactivation, and limited stability. These limitations highlight the need for molecular-level screening of natural chromophores to determine whether their intrinsic electronic and excited-state properties are compatible with DSSC operation.

Among the relatively less explored natural chromophores, shikonin (SKN) and acetylshikonin (ASK) are particularly interesting naphthoquinone derivatives with extended π-conjugation and multiple oxygen-containing functional groups. Their electronic structures give rise to strong visible absorption, while their excited-state behaviour can involve solvent-dependent relaxation and proton-transfer processes. Such competing excited-state pathways may substantially influence their suitability for photovoltaic charge-transfer applications. In contrast, violacein (VLC) and pseudodeoxyviolacein (PDV) are biologically derived indole-based pigments with substantially different conjugated frameworks. VLC is known for its pronounced visible absorption and complex excited-state dynamics, including solvent- and conformation-dependent relaxation. The structural differences between these two pigment families provide an interesting basis for examining how molecular architecture controls DSSC-relevant electronic and optical properties.

Despite extensive investigations of natural dyes for DSSCs, most studies have focused on experimentally extracted pigments or individual pigment families, whereas systematic computational comparisons among structurally distinct natural chromophores remain limited [16–18]. In particular, a consistent quantum chemical assessment of ASK, SKN, PDV, and VLC in terms of frontier molecular orbital (FMO) characteristics, optical transitions, solvent effects, and DSSC-relevant energy-transfer processes has not been sufficiently established**.** It therefore remains unclear how the different molecular architectures influence their energy-level alignment with TiO_2 and I^-/I_3^- redox couple, and which compounds provide the most favorable combination of light harvesting efficiency (LHE) and charge-transfer energetics.

In the present work, density functional theory (DFT) and time dependent DFT (TD-DFT) calculations have been employed to systematically investigate ASK, SKN, PDV, and VLC as prospective natural photosensitizers for DSSCs. Ground-state properties are examined through optimized molecular structures, FMOs, electrostatic potential (ESP) surfaces, and density of states (DOS), while excited-state characteristics are evaluated from absorption energies, oscillator strengths, LHE, and excited-state lifetimes. The analysis is performed in both the gas phase and acetonitrile medium to assess the influence of the dielectric environment. In addition, the calculated frontier energy levels are compared with the TiO_2 conduction-band edge and I^-/I_3^- redox potential to evaluate the thermodynamic feasibility of electron injection and dye regeneration.

The novelty of this study lies in providing a unified electronic-structure and photovoltaic-oriented comparison of two chemically distinct classes of natural pigments. By integrating ground- and excited-state properties with DSSC-relevant energetic descriptors, the study identifies the molecular features that govern the relative suitability of ASK, SKN, PDV, and VLC as sensitizers. The results provide a computational basis for prioritizing these natural chromophores for experimental validation and may contribute to the rational development of bio-derived sensitizers with improved light harvesting and charge-transfer characteristics.

2. Computational Methodology

All quantum chemical calculations were performed using the Gaussian 16W software package (Revision A.03) [19]. The ground-state geometries of ASK, SKN, PDV, and VLC were fully optimized within the framework of DFT, employing the B3LYP hybrid exchange–correlation functional [20, 21] and the 6-311G(d,p) basis set [22]. This computational approach offers a suitable compromise between accuracy and computational efficiency for π-conjugated organic systems. Harmonic vibrational frequency calculations were subsequently conducted at the same level of theory to verify the structural stability of the optimized geometries, with the absence of imaginary frequencies confirming their correspondence to local minima on the potential energy surfaces. FMO analysis, encompassing the highest occupied molecular orbital (HOMO) and lowest unoccupied molecular orbital (LUMO), was performed to investigate the electronic characteristics of the studied compounds. Furthermore, ESP maps were extracted to examine the spatial distribution of electron density and identify electrostatically favorable regions potentially involved in interactions with semiconductor surfaces. The excited-state electronic properties and optical absorption behavior were evaluated using TD-DFT. Gas phase and acetonitrile phase UV–visible absorption spectra were simulated using the long-range-corrected CAM-B3LYP functional [23] in conjunction with the 6-311G(d,p) basis set, which provides an improved description of electronic

134 excitations, particularly those involving charge-transfer character in conjugated molecular systems
135 [23]. Solvent effects arising from acetonitrile were incorporated through the polarizable continuum
136 model (PCM). The CAM-B3LYP functional was selected because of its established capability to
137 describe charge-transfer excitations and provide reliable estimates of excitation energies in
138 conjugated molecular systems [23]. The calculated vertical excitation energies, oscillator
139 strengths, and molecular orbital configuration coefficient (MOCC) were analyzed to characterize
140 the electronic transitions and their contributions to the optical response. The maximum absorption
141 wavelengths (λ_{max}) were identified from the calculated transitions and their oscillator strengths.

142 To assess the photovoltaic potential of the investigated dyes for DSSC applications, several key
143 performance parameters were determined using established theoretical approaches. Among these,
144 the electron injection free energy (ΔG^{inject}) was calculated according to equation (1) [24]:

$$\Delta G^{inject} = E^{dye*} - |E_{CB}| \quad (1)$$

145 Where, E_{CB} is the energy of conduction band edge of TiO_2 and E^{dye*} is the excited-state oxidation
146 potential of the dye which is defined by the equation (2):

$$E^{dye*} = E^{dye} - E^{00} \quad (2)$$

147 Here, E^{dye} is the oxidation potential of the dye in ground-state ($\approx |E_{HOMO}|$), and E^{00} is the TD-
148 DFT calculated excitation energy. Hence, ΔG^{inject} can be stated as below equation (3) [24]:

$$\Delta G^{inject} = E^{dye} - E^{00} - |E_{CB}| \quad (3)$$

149 The dye regeneration free energy (ΔG^{reg}) was determined using the following expression (4) [2]:

$$\Delta G^{reg} = |E_{redox}| - E^{dye} \quad (4)$$

Where, E_{redox} is the redox potential of the I^-/I_3^- electrolyte typically used in DSSC fabrication.

The open-circuit voltage (V_{OC}) was estimated using the empirical relationship proposed by Scharber et al. [25], which relates the HOMO energy level of the dye to the CB energy of the semiconductor (5) [26–28]:

$$V_{OC} = \frac{1}{e}[|E_{HOMO}| - |E_{CB}| - 0.3 \quad (5)$$

Oscillator strength (f) was used to calculate the light-harvesting efficiency (LHE) of the dye using the following equation (6) [9]:

$$LHE = 1 - 10^{-f} \quad (6)$$

Finally, the excited-state lifetime (τ), a key parameter influencing charge recombination dynamics and the photo-physical behavior of the dyes, was estimated using equation (7) [29, 30]:

$$\tau = \frac{1.499}{f E_{ex}^2} \quad (7)$$

Here, E_{ex} is the excitation energy (in cm^{-1} units) of the corresponding excited state.

In addition, the charge shared (ΔN) between the photosensitizer dye and the semiconductor (considered here TiO_2) was assessed as follows [31–33]:

$$\Delta N = \frac{\chi_{TiO_2} - \chi_{dye}}{2\,(\eta_{TiO_2} + \eta_{dye})} \quad (8)$$

Here, χ_{TiO_2} and η_{TiO_2} are the electronegativity and global hardness of the semiconductor TiO_2, respectively and the stated values are 5.58 and 1.58 respectively [34]. Whereas, χ_{dye} and η_{dye} are those of the dyes, respectively.

All calculations were conducted in the gas phase and in acetonitrile phase to elucidate the intrinsic electronic structures and optical properties of the investigated dyes. The combined DFT and TD-DFT approaches provided a theoretical framework for establishing structure–property relationships and evaluating key electronic and photo-physical parameters relevant to the potential photovoltaic performance of these photosensitizers in DSSCs.

3. Results and Discussions

3.1. Optimized molecular structures and geometrical characteristics

The optimized molecular structures of ASK, SKN, PDV, and VLC obtained from the DFT calculations are presented in Figure 1. The optimized geometries show that the four sensitizers possess their characteristic conjugated molecular frameworks, while clear structural differences are evident between the SKN and VLC molecules. ASK and SKN possess a naphthoquinone-based π-conjugated skeleton, whereas PDV and VLC contain extended indole-derived conjugated frameworks. These differences in molecular architecture are important for DSSC applications because the extent and continuity of π-conjugation directly influence electron delocalization, FMO distribution, and the energy required for electronic excitation.

The optimized structures of ASK and SKN show closely related molecular geometries, with their major conjugated frameworks providing an efficient pathway for electronic delocalization. The structural difference between the two molecules is mainly associated with the substituent configuration of the side chain, which can modify the electronic distribution without fundamentally changing the naphthoquinone core. The presence of several oxygen-containing functional groups is also noteworthy because these sites can influence molecular polarity and electrostatic interactions with the surrounding environment. Such structural characteristics may be

advantageous for sensitization by facilitating interaction between the dye and the semiconductor surface. In contrast, PDV and VLC exhibit more extended heteroatom-containing conjugated frameworks. Their relatively large π-electron systems provide greater opportunities for intramolecular electron delocalization across the molecular backbone. This structural feature is particularly relevant to the calculated electronic properties discussed subsequently, as increased conjugation can facilitate smaller electronic excitation energies and shift optical transitions toward longer wavelengths. The optimized geometry of PDV, in particular, is consistent with its substantially extended conjugation that may later cause low-energy electronic transition. VLC also retains an extended conjugated structure, providing a molecular framework capable of supporting strong electronic transitions in the visible region.

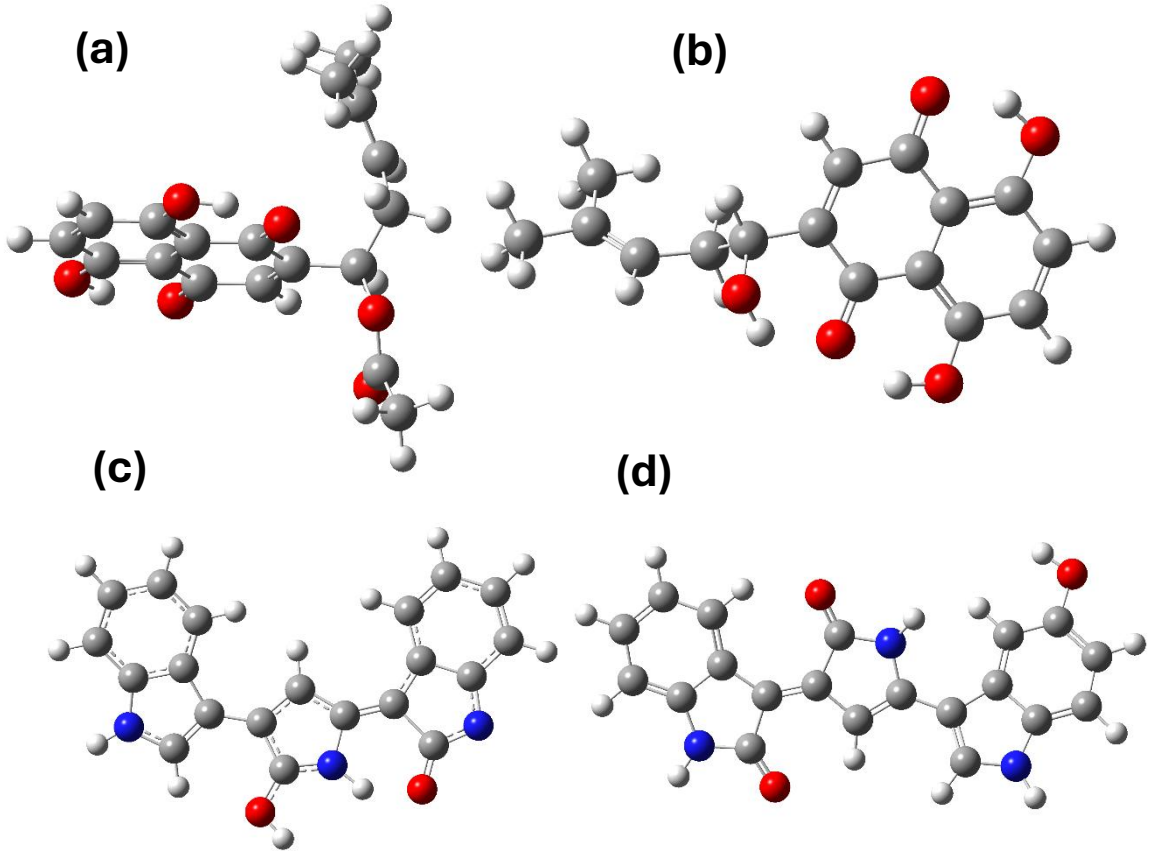

Figure 1: Optimized molecular structures of (a) ASK, (b) SKN, (c) PDV, and (d) VLC obtained using DFT calculations at the B3LYP/6-311G(d,p) level.

From a DSSC perspective, the optimized geometries are important because sensitizer performance depends on the relationship between molecular conformation, conjugation, and electronic-state distribution. A structurally coherent conjugated framework promotes delocalization of the excited electron and influence the spatial separation between electron-donating and electron-accepting regions. The differences observed in Figure 1 therefore provide a structural basis for the variation subsequently obtained in HOMO–LUMO energies, orbital distributions, absorption characteristics, and charge-transfer-related parameters.

3.2 Analyses of Electronic Structures

The electronic structure of a sensitizer dye is one of the most critical factors governing the photovoltaic performance of DSSCs. Efficient DSSC operation requires suitable FMOs alignment, favorable charge distribution, and strong donor–acceptor characteristics to promote visible-light absorption, electron injection into the TiO_2 conduction band, and efficient dye regeneration. To evaluate the DSSC applicability of the investigated dyes, detailed analyses of FMOs, dipole moments, fraction of shared charge, ESP surfaces, and DOS were carried out.

3.2.1. FMO Distribution and Energy-Level Alignment

The FMO distributions provide insights into the electronic structures of the investigated dyes and their potential for electron transfer in DSSCs. Figure 2 and Figure 3 illustrate the HOMO and LUMO distributions of ASK, SKN, PDV, and VLC in the gas phase and acetonitrile medium, respectively. ASK and SKN exhibit frontier orbitals primarily associated with their naphthoquinone-based frameworks, whereas PDV and VLC show orbital distributions extending across their conjugated, nitrogen-containing molecular structures. For ASK, the HOMO and LUMO distributions are concentrated mainly around the quinone-containing region, while SKN exhibits differences in the spatial distribution of its occupied and unoccupied orbitals across the conjugated framework, i. e., the HOMO is distributed mainly on the side chain whereas the LUMO spreads over the napthoquinone moiety. HOMO is mostly located over the unsaturation of the side chain and LUMO is mainly distributed over the quinolone moiety. Such separation of the HOMO and LUMO distribution represents the donor and acceptor regions. PDV and VLC display broader

orbital distributions over their respective molecular backbones, indicating contributions from multiple conjugated regions to the frontier electronic states. These differences suggest that molecular structure influences the electronic transitions of the dyes.

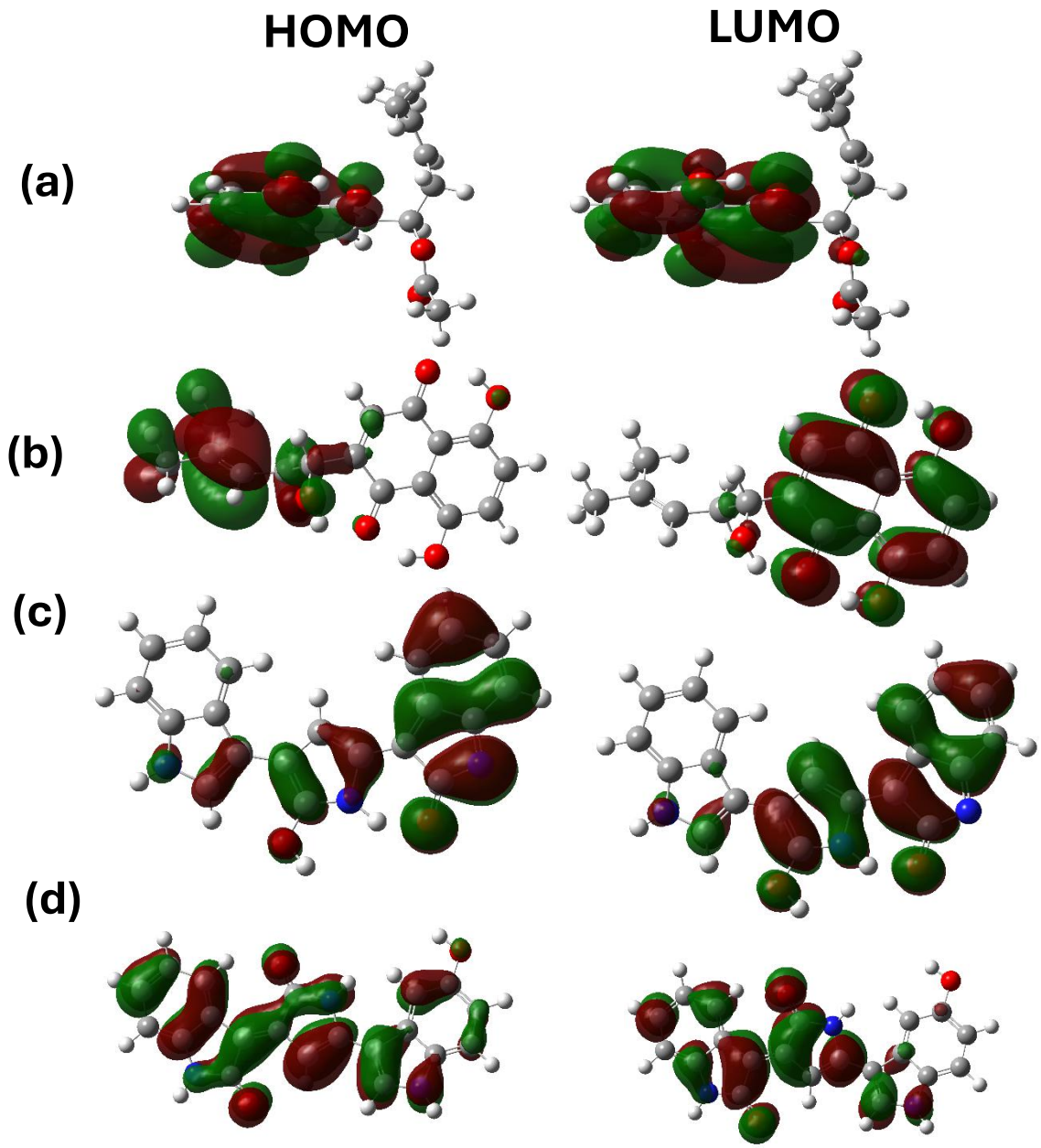

Figure 2: Frontier molecular orbital (HOMO and LUMO) distributions of (a) ASK, (b) SKN, (c) PDV, and (d) VLC calculated using DFT at the B3LYP/6-311G(d,p) level in the gas phase.

The energy-level alignment presented in Figure 4 was evaluated against the TiO_2 conduction-band edge at −4.0 eV and the electrolyte redox potential at −4.8 eV. In both the gas phase and acetonitrile medium, the calculated LUMO energies of the four dyes lie above the TiO_2 conduction-band edge, indicating a favourable energetic arrangement for electron injection following photoexcitation.

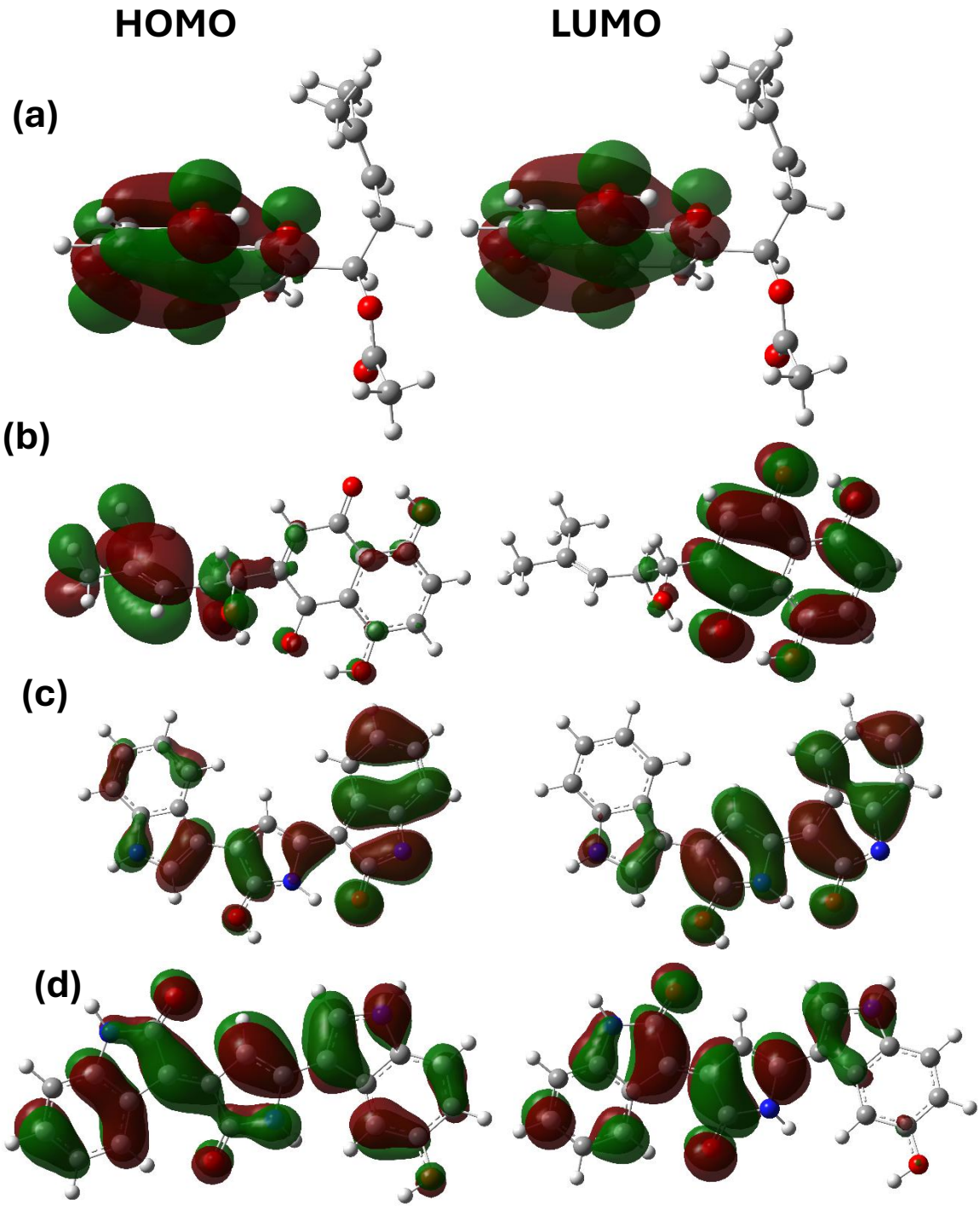

Figure 3: Frontier molecular orbital (HOMO and LUMO) distributions of (a) ASK, (b) SKN, (c) PDV, and (d) VLC calculated at the B3LYP/6-311G(d,p) level in acetonitrile phase.

In the gas phase, the LUMO energies are −3.730 eV for ASK, −3.911 eV for SKN, −3.052 eV for PDV, and −2.469 eV for VLC. The corresponding offsets above the TiO_2 conduction-band edge are 0.270, 0.089, 0.948, and 1.531 eV, respectively. Thus, VLC and PDV have larger energetic offsets for electron injection, whereas SKN has the smallest offset. In acetonitrile, the LUMO energies remain above the conduction-band edge, at −3.730 eV (ASK), −3.770 eV (SKN), −3.178 eV (PDV), and −2.709 eV (VLC), preserving the overall energetic feasibility of electron injection.

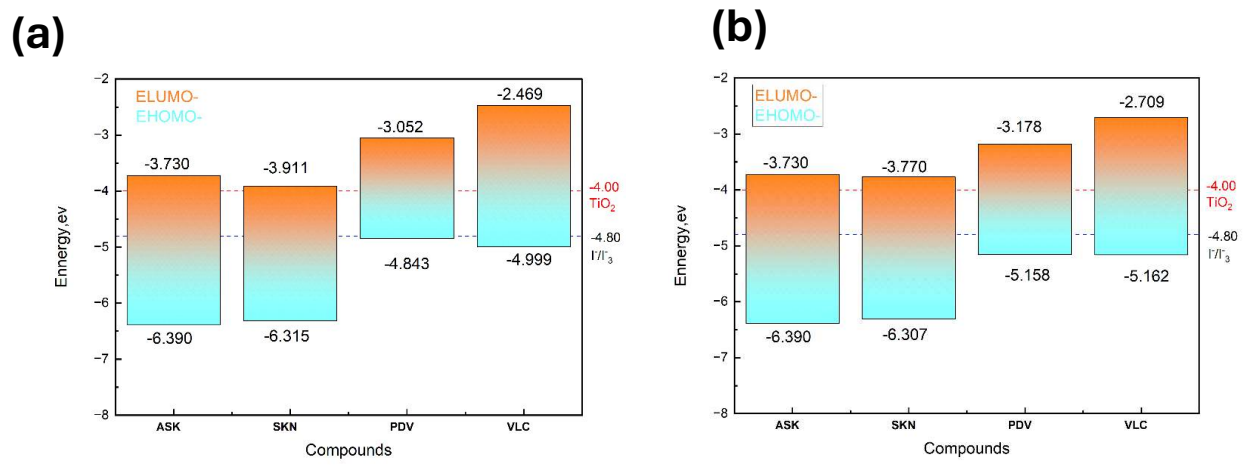

Figure 4: Energy-level alignment of HOMO and LUMO orbitals of ASK, SKN, PDV, and VLC with TiO_2 conduction band edge and I^-/I_3^- redox potential in (a) gas phase and (b) acetonitrile phase.

The HOMO alignment provides complementary information regarding dye regeneration. The calculated HOMO energies of all four dyes lie below the electrolyte redox potential of −4.8 eV, although the energetic separation varies considerably. In the gas phase, ASK (−6.390 eV) and SKN (−6.315 eV) exhibit substantially deeper HOMO levels than PDV (−4.843 eV) and VLC (−4.999 eV). This alignment suggests a greater thermodynamic driving force for regeneration of oxidized ASK and SKN, whereas the smaller energy differences for PDV and VLC indicate comparatively less favourable regeneration energetics. A similar trend is observed in acetonitrile: the deeper HOMO levels of ASK (−6.390 eV) and SKN (−6.307 eV) remain favourable for regeneration, while PDV (−5.158 eV) and VLC (−5.162 eV) exhibit more limited energetic offsets relative to the redox potential. Overall, the FMO distributions and energy-level alignment demonstrate complementary characteristics among the four dyes: PDV and VLC provide larger calculated energetic offsets for electron injection, whereas ASK and SKN exhibit more favourable HOMO alignment for dye regeneration. These findings indicate that the potential of the investigated

natural pigments as DSSC sensitizers must be assessed by considering both injection and regeneration energetics rather than either parameter independently.

3.2.2 Dipole Moments

The dipole moment is an important molecular descriptor that reflects the magnitude of charge separation within a molecule. In DSSCs, it can provide useful insight into molecular polarity, intramolecular charge redistribution, and the possible interaction of a sensitizer with the semiconductor surface. However, the dipole moment alone cannot establish the efficiency of electron injection or predict the overall photovoltaic performance of a dye.

As shown in Figure 5**(a),** the calculated dipole moments vary considerably among the four investigated photosensitizers. In the gas phase, PDV exhibits the highest dipole moment (9.264 D), followed by VLC (3.698 D), ASK (2.382 D), and SKN (2.015 D). This trend indicates that PDV has a substantially greater molecular dipole than the other three dyes, suggesting more pronounced charge separation in its ground-state electronic distribution. The extended conjugated framework and heteroatom-containing structure of PDV may contribute to this behaviour. In contrast, the relatively lower dipole moments of ASK and SKN indicate weaker overall molecular polarity, although this does not necessarily imply unfavourable charge-transfer properties.

The influence of the solvent environment is particularly evident for PDV and VLC. In acetonitrile, their dipole moments increase to 14.157 and 5.201 D, respectively, whereas the value for SKN increases moderately to 2.538 D. ASK retains an essentially unchanged dipole moment of 2.382 D. The substantial increase for PDV suggests that the polar solvent environment modifies its electronic charge distribution more strongly than that of the other dyes. Such solvent-dependent polarization may influence the stabilization of electronic states and the energetics of photoinduced charge transfer under DSSC operating conditions. Nevertheless, a larger ground-state dipole moment does not necessarily guarantee faster electron injection, because injection kinetics also depend on excited-state orbital distribution, energetic alignment, electronic coupling with TiO_2, and the adsorption geometry of the dye.

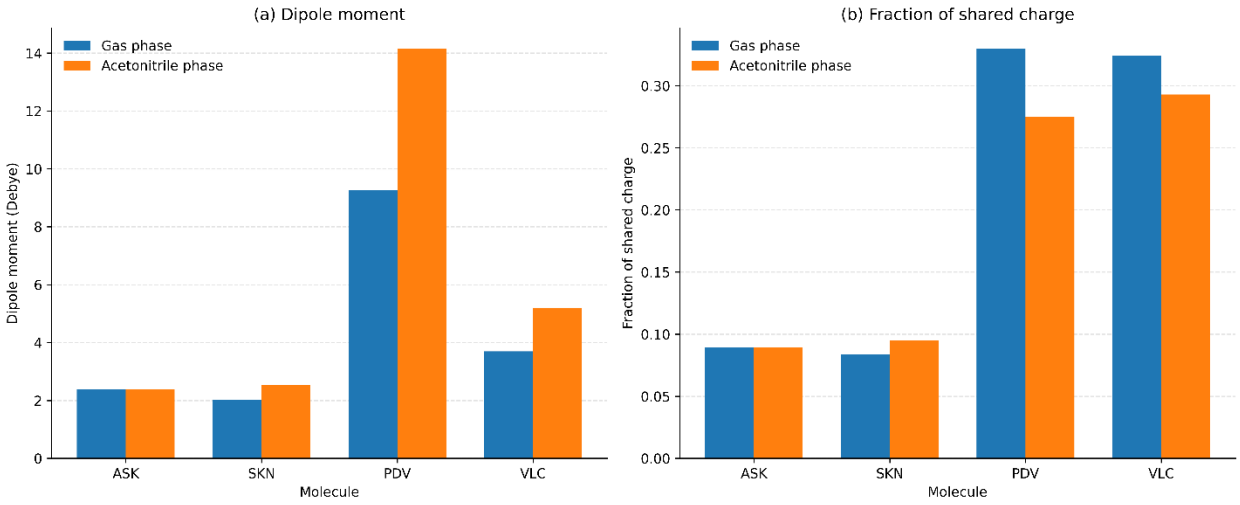

Figure 5: (a) Dipole moments and (b) fraction of shared electrons of the studied photosensitizer molecules.

From a photovoltaic perspective, the high dipole moment of PDV is potentially advantageous because it indicates a pronounced molecular polarity that may be relevant to interfacial charge redistribution. This observation is consistent with the relatively favourable calculated energetic driving force for electron injection reported in Table 2. VLC also exhibits a larger dipole moment than ASK and SKN and has favourable calculated injection energetics. Conversely, although ASK and SKN possess lower dipole moments, their deeper HOMO energy levels suggest more favourable thermodynamic conditions for regeneration by the electrolyte. Therefore, the dipole-moment results highlight different electronic characteristics among the investigated dyes rather than establishing a definitive performance ranking. Overall, PDV appears particularly interesting in terms of molecular polarity, while the DSSC suitability of the four dyes should be assessed in conjunction with their charge-transfer descriptors, energy-level alignment, and optical properties.

3.2.3 Analysis of the Fraction of Shared Charge Transferred

The fractional electron-transfer descriptor (ΔN) provides a complementary perspective on the potential charge-transfer behaviour of the investigated sensitizers. In this study, ΔN was calculated from the electronegativity difference and the combined global hardness of the dye and TiO_2 using Equation (8). Within this theoretical framework, a larger positive ΔN indicates a greater predicted tendency for electron redistribution from the dye towards TiO_2. This parameter is useful for comparative screening of the studied dye molecules, although it should not be interpreted as a direct measurement of the number of electrons injected during actual DSSC operation.

As illustrated in Figure 5(b) and reported in Table S1, PDV and VLC exhibit considerably higher fractional electron-transfer values than ASK and SKN in the gas phase. The calculated values are 0.330 for PDV and 0.324 for VLC, compared with 0.089 for ASK and 0.084 for SKN. These results suggest that the two indole-based pigments have a greater predicted tendency for dye-to-semiconductor charge redistribution within the adopted model. Their relatively higher values may be associated with their distinct electronic structures and lower calculated global hardnesses, which indicate greater electronic softness. In particular, the extended conjugated frameworks of PDV and VLC may facilitate electronic delocalization, although the magnitude of interfacial electron injection ultimately depends on the electronic coupling between the excited dye and the semiconductor.

The solvent-phase results reveal a change in the relative charge-transfer descriptors. In acetonitrile, the calculated ΔN values are 0.089 for ASK, 0.095 for SKN, 0.275 for PDV, and 0.293 for VLC. Thus, PDV and VLC continue to exhibit higher predicted electron-transfer tendencies than ASK and SKN, although their values decrease compared with those calculated in the gas phase. VLC becomes the highest-ranking dye in acetonitrile, whereas PDV retains the highest value in the gas phase. This variation indicates that the solvent environment can influence the relative electronic response of the sensitizers. The comparatively small change in ASK and the modest increase in SKN further suggest that the predicted charge redistribution of these naphthoquinone derivatives is less sensitive to the solvent within the present model.

These findings have important implications for evaluating the dyes as DSSC sensitizers. The relatively high ΔN values of PDV and VLC, combined with their favourable calculated LUMO alignment above the TiO_2 conduction-band edge, identify them as promising candidates for further investigation of electron injection. As reported in Figure 4, ASK and SKN possess deeper HOMO energy levels, indicating more favourable calculated regeneration energetics than those of PDV and VLC. Consequently, the lower ΔN values of ASK and SKN do not exclude them from DSSC applications; their potential advantages in dye regeneration may partly compensate for their less favourable predicted charge redistribution.

Taken together, the results demonstrate that the four natural pigments exhibit complementary electronic characteristics. PDV shows the highest calculated dipole moment and fractional

electron-transfer value in the gas phase, whereas VLC exhibits the highest fractional electron-transfer value in acetonitrile. These findings support prioritizing PDV and VLC for further investigation of interfacial charge transfer, while ASK and SKN remain relevant candidates because of their favourable regeneration energetics.

3.2.4. Electrostatic Potential Surface Analysis

The electrostatic potential (ESP) surfaces presented in Figure 6 illustrate the spatial distribution of electrostatic potential across the molecular frameworks of ASK, SKN, PDV, and VLC. All four molecules exhibit an irregular electrostatic potential distributions, reflecting differences in their molecular structures and heteroatom-containing functional groups. For ASK and SKN, the oxygen-containing quinone groups are associated with localized regions of electrostatic potential, indicating sites that may participate in intermolecular interactions. Similarly, PDV and VLC exhibit heterogeneous potential distributions across their conjugated, nitrogen-containing frameworks, with contributions from their oxygen- and nitrogen-containing functional groups. These differences indicate that the molecular structures influence the location and distribution of electrostatically distinct regions, which may affect interactions with the surrounding environment and the TiO_2 semiconductor surface.

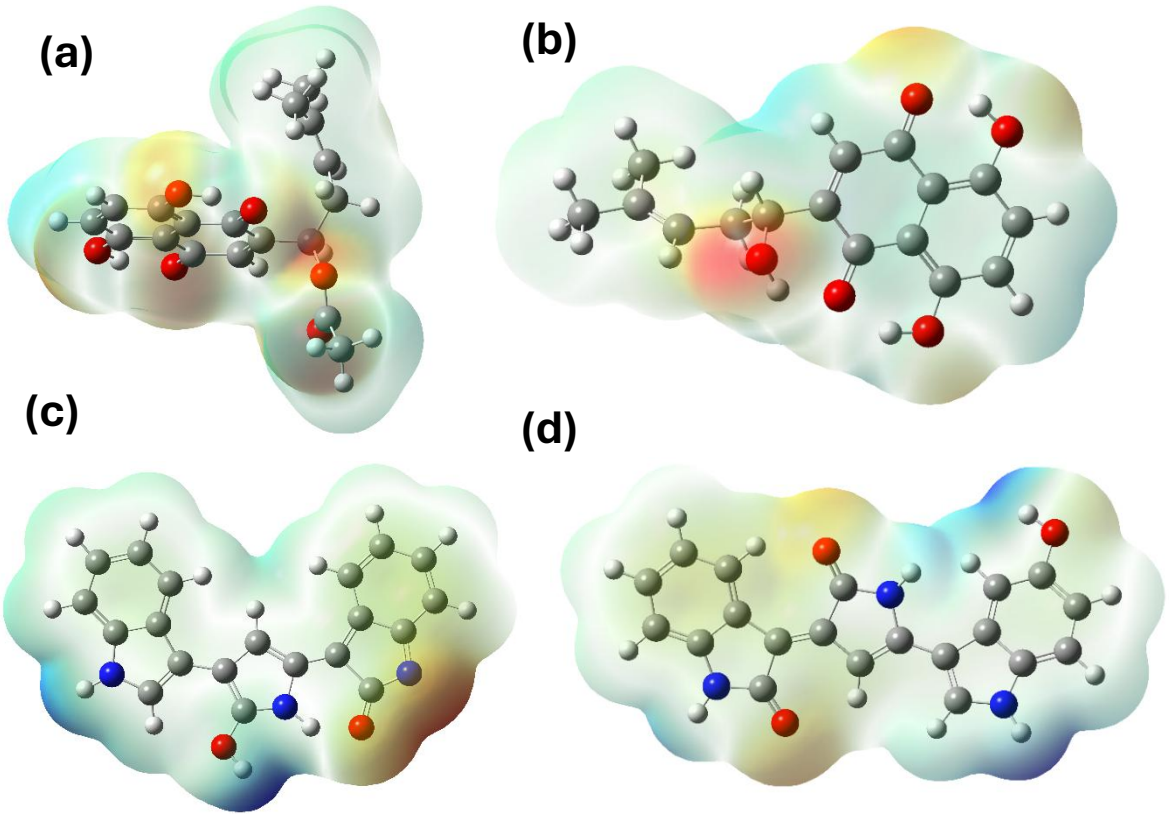

Figure 6: Electrostatic potential (ESP) surfaces of (a) ASK, (b) SKN, (c) PDV, and (d) VLC in gas phase.

From the perspective of DSSC applications, the ESP distributions provide preliminary insight into potential dye–semiconductor interactions and the identification of regions that may be relevant to surface adsorption. The localized electrostatic features of ASK and SKN may contribute to interactions involving their oxygen-containing groups, whereas the more extended conjugated frameworks of PDV and VLC offer different distributions of electrostatic potential across their molecular backbones. These characteristics may influence molecular orientation and interfacial electronic interactions, which are relevant to electron injection from the photoexcited dye into the TiO_2 conduction band. However, the ESP surfaces alone cannot establish adsorption strength, binding stability, or electron-injection efficiency, particularly because effective dye anchoring depends on the accessibility and chemical suitability of specific functional groups. Therefore, the ESP results should be considered alongside the frontier molecular orbital distributions, energy-level alignment, and fractional electron-transfer descriptors to provide a more comprehensive assessment of the potential suitability of the four natural pigments as DSSC sensitizers.

3.2.5. Density of States Analysis

The total density of states (TDOS) profiles presented in Figure 7 and Figure 8 provide insight into the distribution of electronic states and the frontier energy levels of ASK, SKN, PDV, and VLC in the gas phase and acetonitrile medium, respectively. The distributions of electronic states differ among the four sensitizers, reflecting their distinct molecular structures and electronic configurations. The calculated HOMO–LUMO energy gaps provide a useful basis for comparing their electronic characteristics.

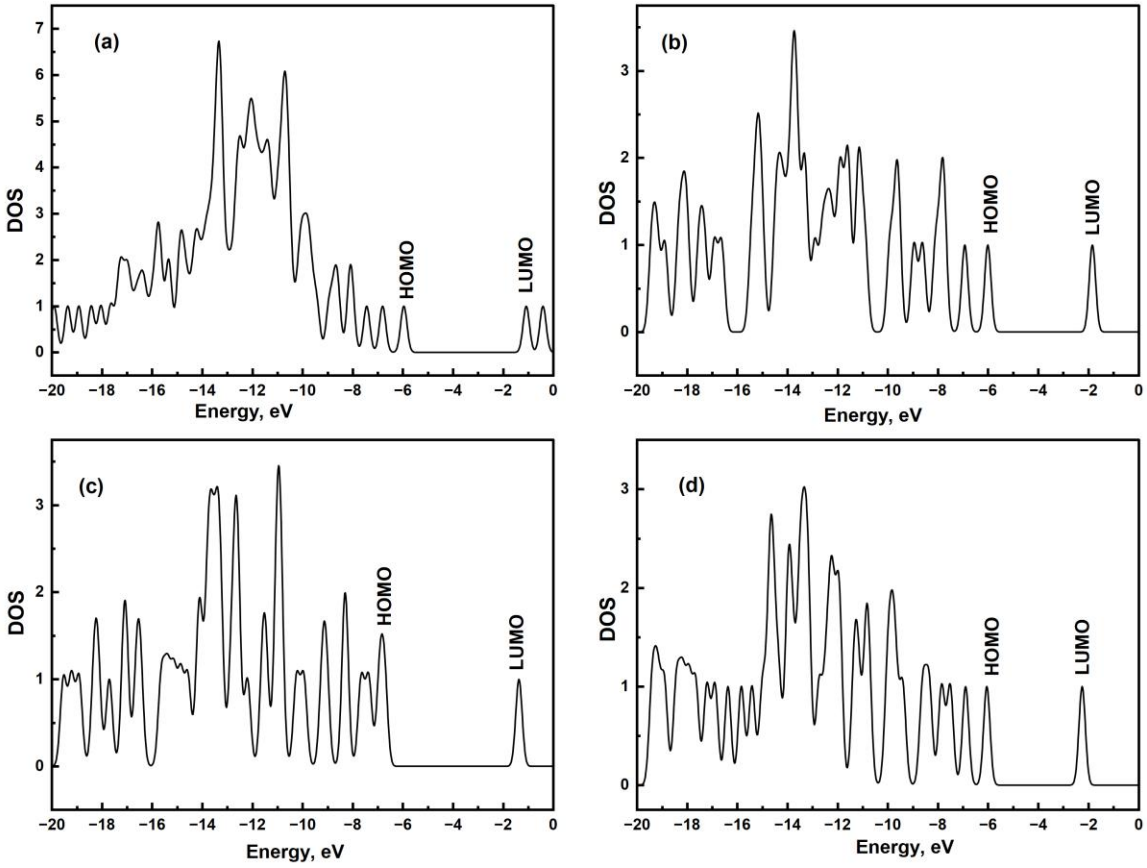

Figure 7: Total density of states (TDOS) profiles of (a) ASK, (b) SKN, (c) PDV, and (d) VLC in the gas phase.

In the gas phase, the energy gaps follow the order PDV (1.791 eV) < SKN (2.404 eV) < VLC (2.530 eV) < ASK (2.660 eV), whereas in acetonitrile, the corresponding values are 1.980, 2.537, 2.453, and 2.660 eV, respectively. PDV therefore exhibits the smallest energy gap in both environments, suggesting that its frontier electronic states are more closely spaced than those of the other investigated dyes. This characteristic may favour electronic excitation and is consistent with its calculated low-energy absorption transition. By contrast, ASK exhibits the largest energy

gap in both phases, indicating a comparatively wider separation between its occupied and unoccupied frontier orbitals. The differences in the TDOS profiles and frontier energy gaps demonstrate that the electronic properties of the sensitizers are strongly influenced by their molecular frameworks.

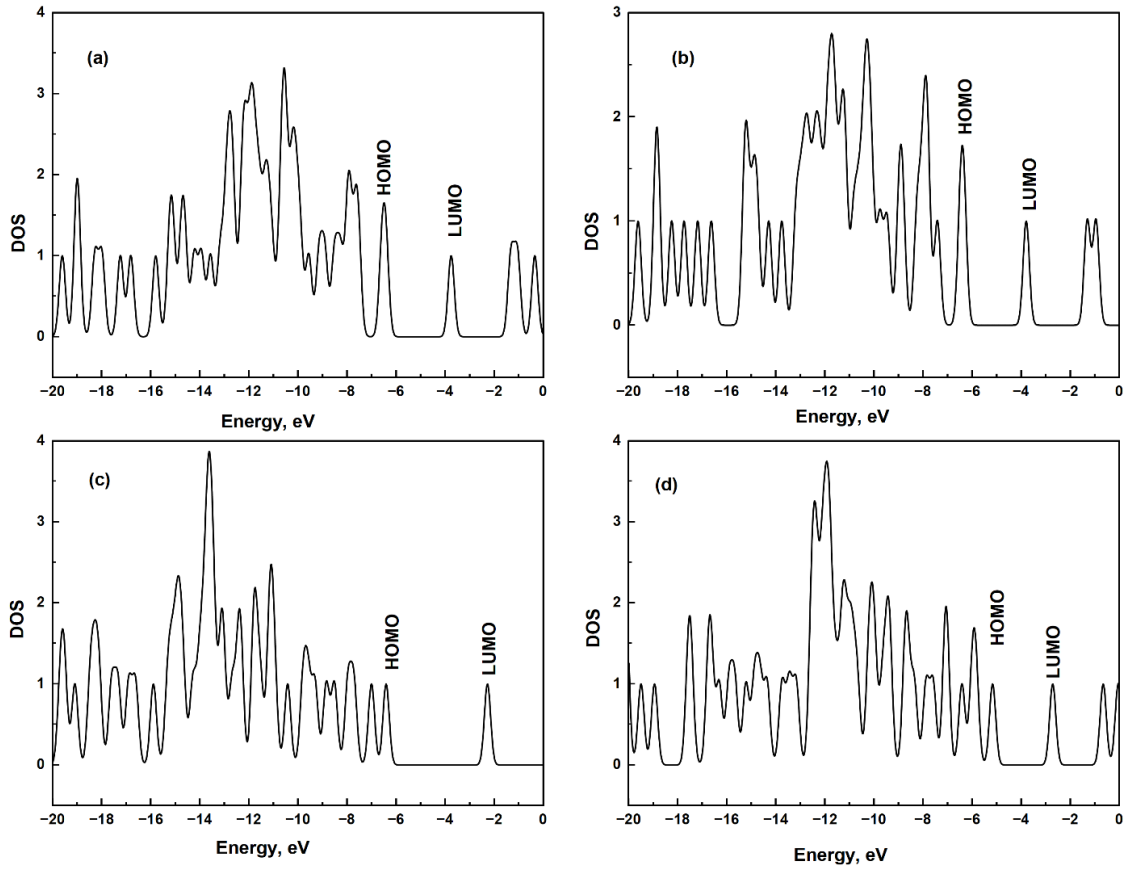

Figure 8: Total density of states (TDOS) profiles of (a) ASK), (b) SKN, (c) PDV, and (d) VLC in acetonitrile phase

From the perspective of DSSC applications, the TDOS results help explain the relative electronic characteristics of the investigated sensitizers and complement the frontier molecular orbital and optical absorption analyses. The smaller energy gap of PDV may be beneficial for accessing low-energy electronic excitations, while the relatively small gap of VLC in acetonitrile (2.453 eV) also indicates favourable frontier-state spacing compared with ASK and SKN under the same conditions. However, a narrow HOMO–LUMO gap alone does not establish efficient electron injection into the TiO_2 conduction band or guarantee enhanced photovoltaic performance. These processes also depend on the excited-state energy, the alignment of the dye energy levels with the

semiconductor and electrolyte redox potential, and the electronic coupling at the dye–semiconductor interface. Notably, the changes in the calculated energy gaps between the gas and acetonitrile phases indicate that the solvent environment can modify the relative electronic properties of the dyes, particularly SKN and PDV. Overall, the TDOS analysis identifies PDV as a particularly interesting candidate for further investigation because of its consistently smaller energy gap, while the suitability of ASK, SKN, and VLC should be assessed by considering their complementary optical and charge-transfer characteristics. These findings provide a theoretical basis for prioritizing the four natural pigments for further experimental evaluation as potential DSSC sensitizers.

3.3. Optical Properties and Simulated UV–Visible Spectra Analysis

The optical absorption characteristics of photosensitizer molecules play a crucial role in determining their light-harvesting capability and photovoltaic suitability for DSSCs. Strong absorption across the visible and near-infrared regions is desirable for efficient utilization of incident solar radiation. To evaluate the optical properties of ASK, SKN, PDV, and VLC, TD-DFT calculations were performed to determine their excitation energies, maximum absorption wavelengths (λ_{max}), oscillator strengths (*f*), and dominant electronic transitions. The calculated parameters are summarized in Table 1, while the simulated UV–visible absorption spectra in the gas phase and acetonitrile medium are illustrated in Figure 9 and Figure 10, respectively.

Table 1: TD-DFT calculated excitation properties of ASK, SKN, PDV, and VLC in gas phase and acetonitrile phase.

Phase	Compound	Excitation energy, E_{ex} (eV)	λ_{max} (nm)	Oscillator strength (f)	Dominant transition	MO configuration coefficient
Gas	ASK	2.7714	447.38	0.1640	HOMO → LUMO	0.70627
	SKN	2.7222	455.46	0.1809	HOMO → LUMO	0.63987
	PDV	1.6165	767.02	0.1732	HOMO → LUMO	0.5887
	VLC	2.5426	487.63	0.6071	HOMO → LUMO	0.69291
Acetonitrile	ASK	2.7115	457.26	0.1994	HOMO → LUMO	0.70604
	SKN	2.7073	457.97	0.2209	HOMO → LUMO	0.68983
	PDV	1.6852	735.71	0.1632	HOMO → LUMO	0.65161
	VLC	2.4294	510.35	0.7115	HOMO → LUMO	0.68961

As presented in Table 1 and Figure 9, the investigated dyes exhibit distinct absorption characteristics associated with their molecular structures. In the gas phase, ASK and SKN display absorption maxima at 447.38 and 455.46 nm, corresponding to excitation energies of 2.7714 and 2.7222 eV, respectively. Their relatively close absorption wavelengths reflect the similarities between their naphthoquinone-based conjugated frameworks.

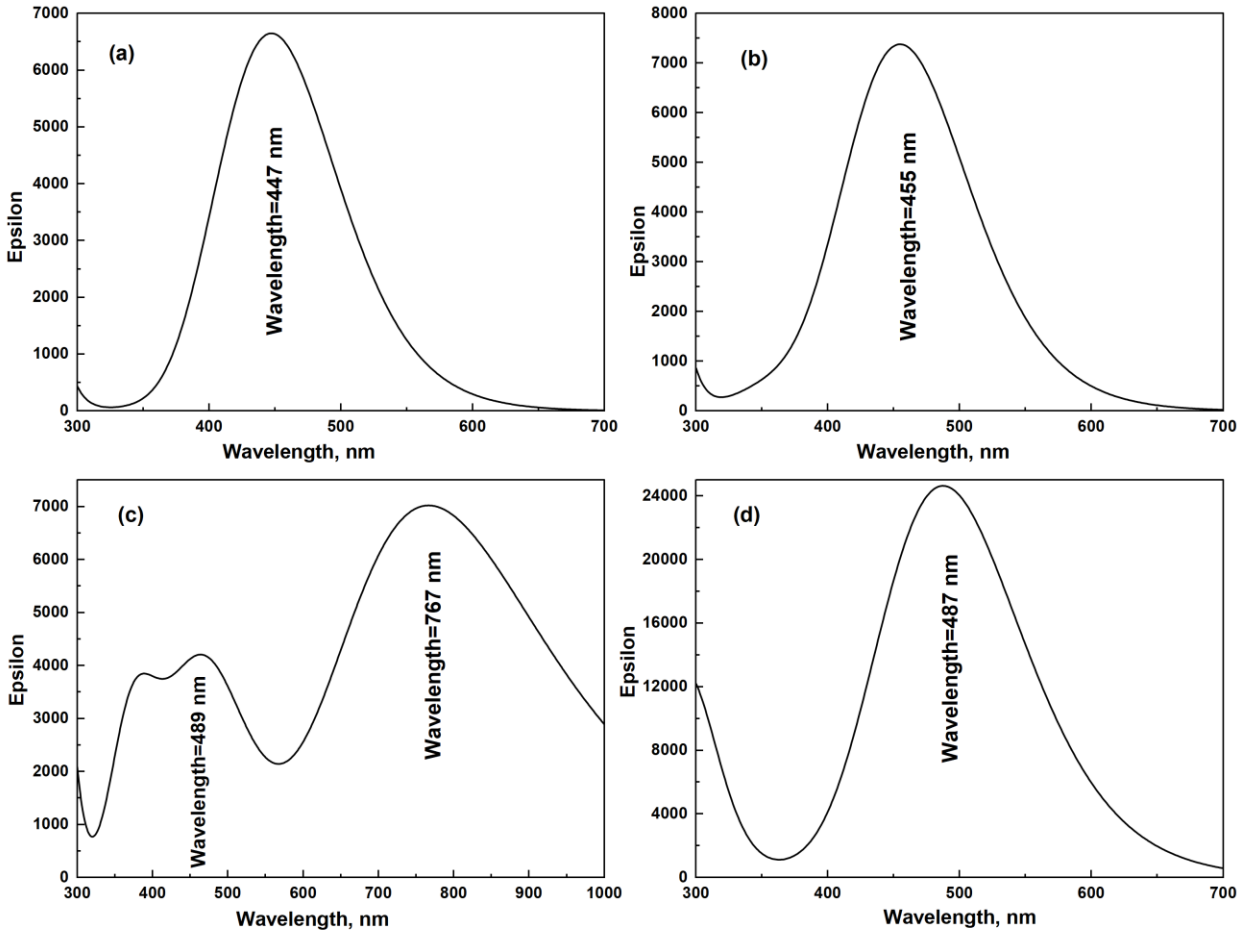

Figure 9: Simulated UV–visible absorption spectra of (a) ASK, (b) SKN, (c) PDV, and (d) VLC in the gas phase obtained from TD-DFT calculations.

The corresponding oscillator strengths of 0.1640 and 0.1809 indicate moderately allowed electronic transitions, suggesting their potential for harvesting light predominantly in the blue region of the visible spectrum. In contrast, PDV exhibits the most pronounced red-shifted absorption, with λ_{max} of 767.02 nm and the lowest excitation energy of 1.6165 eV. This

characteristic is consistent with its comparatively narrow HOMO–LUMO energy gap and indicates its ability to access lower-energy photons in the red and near-infrared regions. However, its moderate oscillator strength (0.1732) suggests that the extended spectral coverage is accompanied by a relatively weaker transition intensity. VLC, meanwhile, exhibits an absorption maximum at 487.63 nm with an excitation energy of 2.5426 eV and the highest gas-phase oscillator strength (0.6071), indicating substantially stronger optical activity within the visible region.

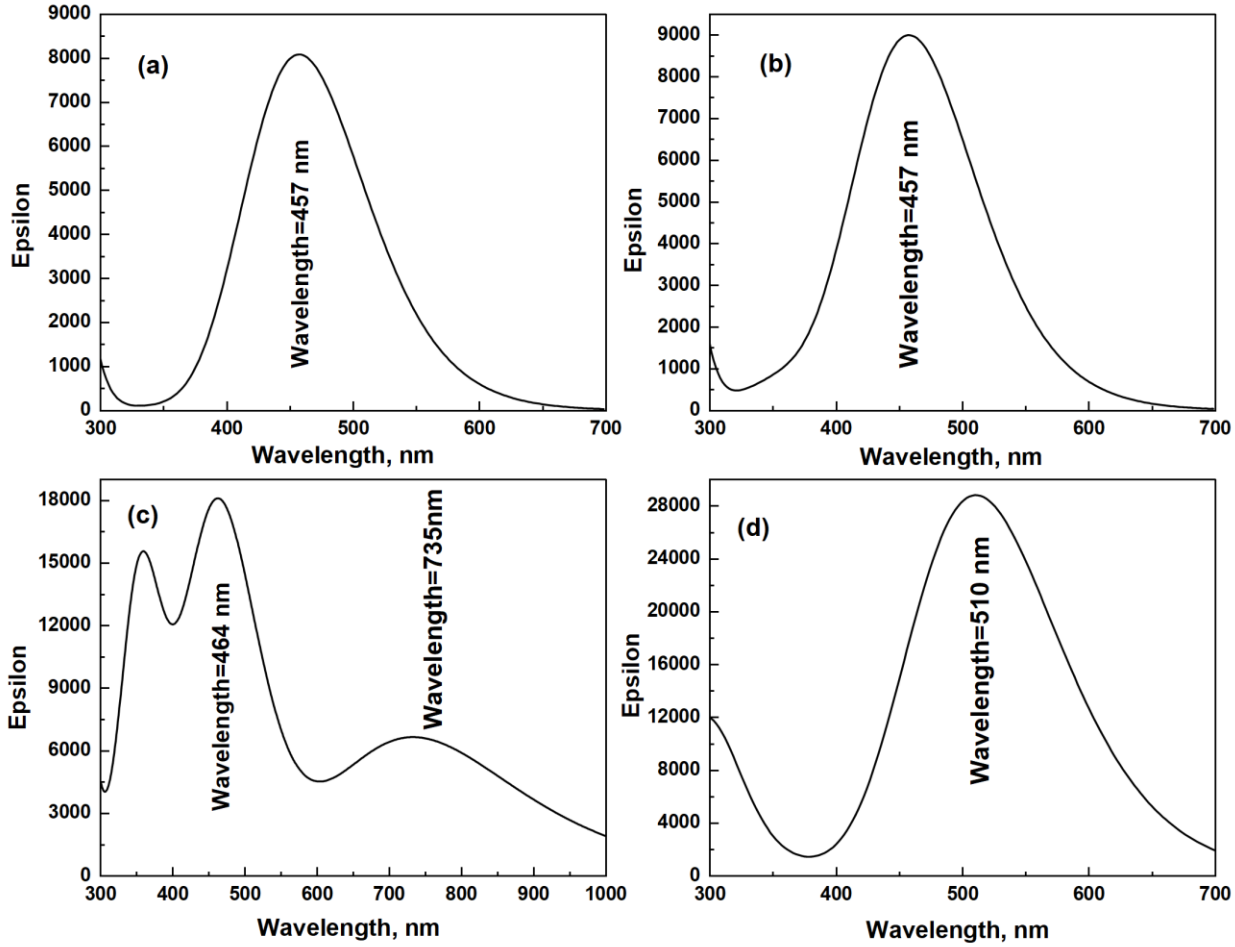

Figure 10: Simulated UV–visible absorption spectra of (a) ASK, (b) SKN, (c) PDV, and (d) VLC in acetonitrile phase obtained from TD-DFT calculations

The acetonitrile-phase results in Table 1 and Figure 10 reveal solvent-dependent changes in the absorption characteristics. ASK and SKN exhibit modest bathochromic shifts to 457.26 and 457.97 nm, respectively, accompanied by increased oscillator strengths of 0.1994 and 0.2209. These changes suggest enhanced transition strengths in the polar solvent environment. Similarly, VLC undergoes a red shift from 487.63 to 510.35 nm, with its oscillator strength increasing from 0.6071

to 0.7115, the highest among the investigated sensitizers. This enhancement is consistent with its calculated light-harvesting efficiency of 0.806 in acetonitrile (Table 2), indicating favourable optical characteristics for visible-light absorption. Conversely, PDV exhibits a hypsochromic shift from 767.02 to 735.71 nm, accompanied by a slight reduction in oscillator strength from 0.1732 to 0.1632. Nevertheless, its simulated spectrum retains substantial long-wavelength absorption, highlighting its potential for extending light harvesting towards the near-infrared region. These solvent-induced spectral shifts indicate differences in the relative stabilization of the ground and excited electronic states.

The electronic transition analysis further reveals that the reported low-energy excitations of all four dyes are dominated by HOMO → LUMO transitions in both environments, with molecular orbital configuration coefficients ranging from 0.58870 to 0.70627 in the gas phase and from 0.65161 to 0.70604 in acetonitrile. These findings indicate that the frontier molecular orbitals contribute substantially to the observed absorption bands, establishing a relationship between their electronic structures and optical responses. From a DSSC perspective, PDV offers the advantage of long-wavelength photon absorption, whereas VLC exhibits the strongest calculated optical transitions and highest light-harvesting efficiency. ASK and SKN demonstrate comparatively weaker, shorter-wavelength absorption but retain potential relevance because of their favourable regeneration energetics. Overall, the results identify PDV and VLC as promising photosensitizer candidates with complementary optical characteristics. However, their practical photovoltaic performance will also depend on efficient electron injection into TiO_2, dye regeneration, and suppression of charge recombination, requiring further experimental validation.

3.4. Photovoltaic Performance Analysis

The photovoltaic suitability of photosensitizers in DSSCs is governed by their electron injection and dye regeneration energetics, light-harvesting capability, and excited-state characteristics. To evaluate these properties, the electron injection free energy (ΔG^{inject}), dye regeneration free energy (ΔG^{reg}), estimated open-circuit voltage (V_{OC}), light-harvesting efficiency (LHE), and excited-state lifetime (τ) of ASK, SKN, PDV, and VLC were calculated in the gas phase and acetonitrile medium. The corresponding photovoltaic descriptors are presented in Table 2, providing a

comparative assessment of the potential performance of these natural pigments as DSSC sensitizers.

Table 2: Calculated DSSC-related photovoltaic descriptors of ASK, SKN, PDV, and VLC in gas phase and acetonitrile phase

	Dye	E_{HOMO} (eV)	E_{LUMO} (eV)	E^{00} (eV)	E^{dye} (eV)	E^{dye*} (eV)	ΔG^{inject} (eV)	ΔG^{reg} (eV)	V_{OC} (V)	LHE	τ (ns)
Gas	ASK	−6.390	−3.730	2.771	6.390	3.619	-0.381	-1.590	2.090	0.315	18.327
	SKN	−6.315	−3.911	2.722	6.315	3.593	-0.407	-1.515	2.015	0.341	17.220
	PDV	-4.843	-3.052	1.617	4.843	3.227	-0.774	-0.043	0.543	0.329	51.006
	VLC	−4.999	−2.469	2.543	4.999	2.456	-1.544	-0.199	0.699	0.753	5.882
Acetonitrile	ASK	−6.390	−3.730	2.712	6.390	3.679	-0.322	-1.590	2.090	0.368	15.746
	SKN	−6.307	−3.770	2.707	6.307	3.600	-0.400	-1.507	2.007	0.399	14.258
	PDV	-5.158	-3.178	1.685	5.158	3.473	-0.527	-0.358	0.858	0.313	49.808
	VLC	−5.162	−2.709	2.429	5.162	2.733	-1.267	-0.362	0.862	0.806	5.497

The ΔG^{inject} provides a thermodynamic measure of the feasibility of electron transfer from the photoexcited dye to the TiO_2 conduction band. As shown in Table 2, the studied sensitizers exhibit negative ΔG^{inject} values in both environments, indicating thermodynamically favourable electron injection within the adopted computational framework. In the gas phase, VLC exhibits the most negative ΔG^{inject} (−1.544 eV), followed by PDV (−0.774 eV), SKN (−0.407 eV), and ASK (−0.381 eV). A similar trend is observed in acetonitrile, where the corresponding values are −1.267, −0.527, −0.400, and −0.322 eV, respectively. The greater negative magnitudes for VLC and PDV indicate stronger thermodynamic driving forces for electron injection than those of ASK and SKN. Notably, VLC retains the strongest injection driving force despite the solvent-induced reduction in its magnitude, suggesting favourable excited-state energetics for electron transfer. However, actual electron injection efficiency also depends on dye adsorption geometry and electronic coupling with the semiconductor surface.

Efficient dye regeneration is equally important for sustaining the photovoltaic cycle by restoring the oxidized sensitizer through electron transfer from the redox electrolyte. The calculated ΔG^{reg} values remain negative for all four dyes, although their magnitudes vary substantially. In the gas phase, ASK and SKN exhibit markedly negative values of −1.590 and −1.515 eV, respectively,

compared with −0.043 eV for PDV and −0.199 eV for VLC. In acetonitrile, the corresponding values are −1.590, −1.507, −0.358, and −0.362 eV. The greater negative magnitudes observed for ASK and SKN indicate stronger thermodynamic driving forces for dye regeneration, consistent with their deeper HOMO energy levels relative to the I^-/I_3^- redox potential. Conversely, the smaller regeneration driving forces of PDV and VLC, particularly in the gas phase, suggest that regeneration could be comparatively less favourable for these dyes. Thus, the calculated energetics reveal a trade-off between electron injection and dye regeneration, emphasizing the importance of balancing both processes rather than optimizing either parameter independently.

The estimated open-circuit voltage (V_{OC}) provides an additional theoretical descriptor for comparing the photovoltaic characteristics of the investigated sensitizers. According to Table 2, ASK exhibits the highest calculated V_{OC} of 2.090 V in both environments, closely followed by SKN with values of 2.015 V in the gas phase and 2.007 V in acetonitrile. In contrast, PDV and VLC exhibit considerably lower values of 0.543 and 0.699 V in the gas phase, increasing to 0.858 and 0.862 V in acetonitrile, respectively. These results indicate that ASK and SKN possess more favourable voltage-related descriptors within the adopted theoretical model, primarily associated with their deeper HOMO energy levels. However, these estimated values should not be interpreted as directly achievable device voltages, since the actual V_{OC} is influenced by the electron quasi-Fermi level of TiO_2, the electrolyte redox potential, and interfacial recombination dynamics.

The light LHE and τ further characterize the optical and photophysical behaviour of the investigated dyes. VLC exhibits the highest LHE values of 0.753 and 0.806 in the gas phase and acetonitrile, respectively, consistent with its strong oscillator strengths and prominent visible-light absorption reported in Table 1 and Figure 9 and Figure 10. In comparison, ASK, SKN, and PDV exhibit relatively lower LHE values of 0.315–0.368, 0.341–0.399, and 0.313–0.329, respectively, across the two environments. Although PDV demonstrates comparatively moderate light-harvesting efficiency, its pronounced long-wavelength absorption provides a complementary advantage for utilizing lower-energy photons. Regarding excited-state lifetime, PDV exhibits the longest estimated values of 51.006 ns in the gas phase and 49.808 ns in acetonitrile, followed by ASK (18.327 and 15.746 ns) and SKN (17.220 and 14.258 ns), whereas VLC displays the shortest lifetimes of 5.882 and 5.497 ns, respectively. The substantially longer estimated lifetime of PDV suggests a potentially favourable time window for interfacial electron transfer. However, these

calculated lifetimes primarily reflect radiative-transition characteristics and do not directly account for nonradiative deactivation or electron injection kinetics.

4. Conclusion

In this study, the electronic structures, optical characteristics, and photovoltaic properties of four natural photosensitizers, ASK, SKN, PDV, and VLC, were systematically investigated using DFT and TD-DFT calculations to assess their potential applications in DSSCs. The results revealed distinct structure–property relationships and solvent-dependent electronic responses that influence their photovoltaic suitability. PDV exhibited the narrowest HOMO–LUMO energy gaps (1.791–1.980 eV) and the most red-shifted absorption maxima (735.71–767.02 nm), indicating favourable near-infrared light-harvesting potential. In contrast, VLC demonstrated the highest oscillator strengths (0.6071–0.7115), light-harvesting efficiencies (0.753–0.806), and electron injection driving forces (−1.544 to −1.267 eV), highlighting its promising optical and charge-transfer characteristics. PDV also possessed the longest estimated radiative lifetime (49.808–51.006 ns), suggesting potentially favourable excited-state persistence. Meanwhile, ASK and SKN exhibited stronger dye regeneration driving forces and higher theoretical voltage-related descriptors, reflecting their favourable occupied orbital energetics. Although all four dyes demonstrated thermodynamically feasible electron injection and regeneration, their contrasting characteristics indicate that photovoltaic suitability depends on balancing light harvesting, charge injection, and dye regeneration. Overall, VLC and PDV emerged as particularly promising natural sensitizers, providing a theoretical foundation for further molecular optimization and experimental validation of sustainable DSSC technologies.

Funding

The authors declare that no funds, grants, or other support were received during the preparation of this manuscript.

CRediT statement

Shahriar Siam: DFT calculation, Data curation, Formal analysis, Visualization, Writing original draft, Editing; Apel Mahamud Rabby: Conceptualization, Methodology, Resources, DFT calculation, Editing; Jewel Hossen: Conceptualization, Methodology, Resources, DFT calculation, Data curation, Formal analysis, Visualization, Writing- original draft, Editing, Review, Revising the original draft; Tanu Dey: Data curation, Visualization; Md. Tanvir Rashid Rezvi: Revising the original draft; Shafikul Islam: Revising the original draft.

Acknowledgements

Authors did not received any financial support for this research work.

Data Availability Statement

All the data are provided in the manuscript and supplementary file.

Declarations

Consent for publication: If this manuscript is accepted for publication in this journal, we would not withdraw it.

Declaration of AI-assisted technologies used in this work: During the preparation of this manuscript, the authors used online AI-assisted tools to enhance the clarity, readability, and overall flow of the text. The authors subsequently reviewed, revised, and verified the content as necessary and take full responsibility for the accuracy, integrity, and final published version of the manuscript.

Conflict of interest statement: There are no conflicts of interest to declare.

References

1. Azaid A, Raftani M, Alaqarbeh M, et al (2022) New organic dye-sensitized solar cells based on the D–A–π–A structure for efficient DSSCs: DFT/TD-DFT investigations. RSC Adv 12:30626–30638. https://doi.org/10.1039/D2RA05297K

2. Daeneke T, Mozer AJ, Uemura Y, et al (2012) Dye Regeneration Kinetics in Dye-Sensitized Solar Cells. J Am Chem Soc 134:16925–16928. https://doi.org/10.1021/ja3054578

3. Grätzel M (2003) Dye-sensitized solar cells. J Photochem Photobiol C Photochem Rev 4:145–153. https://doi.org/10.1016/S1389-5567(03)00026-1

4. Hagfeldt A, Boschloo G, Sun L, et al (2010) Dye-Sensitized Solar Cells. Chem Rev 110:6595–6663. https://doi.org/10.1021/cr900356p

5. Hardin BE, Snaith HJ, McGehee MD (2012) The renaissance of dye-sensitized solar cells. Nat Photonics 6:162–169. https://doi.org/10.1038/nphoton.2012.22

6. Preat J, Michaux C, Jacquemin D, Perpète EA (2009) Enhanced Efficiency of Organic Dye-Sensitized Solar Cells: Triphenylamine Derivatives. J Phys Chem C 113:16821–16833. https://doi.org/10.1021/jp904946a

7. Daeneke T, Mozer AJ, Uemura Y, et al (2012) Dye Regeneration Kinetics in Dye-Sensitized Solar Cells. J Am Chem Soc 134:16925–16928. https://doi.org/10.1021/ja3054578

8. Dutta A, Gohain B, Trang TT, et al (2025) Application of natural photosensitizers in dye-sensitized solar cells: opportunities, challenges, and future outlook. Photochem Photobiol Sci 24:1443–1488. https://doi.org/10.1007/s43630-025-00762-3

9. Sharma K, Sharma V, Sharma SS (2018) Dye-Sensitized Solar Cells: Fundamentals and Current Status. Nanoscale Res Lett 13:381. https://doi.org/10.1186/s11671-018-2760-6

10. Debnath A, Bhattacharjee SK, Sutradhar R, et al (2024) A review on Natural dyes as a sensitizer in dye- dye-sensitized solar cell. Interactions 245:325. https://doi.org/10.1007/s10751-024-02172-w

11. Dhorkule M, Lamrood P, Ralegankar S, et al (2024) Unveiling the Efficiency of Dye-Sensitized Solar Cells: A Journey from Synthetic to Natural Dyes. ES Food Agrofor Volume 16 (June 2024):1086

12. de Souza Farias SA, da Costa KS, Martins JBL (2021) Analysis of Conformational, Structural, Magnetic, and Electronic Properties Related to Antioxidant Activity: Revisiting Flavan, Anthocyanidin, Flavanone, Flavonol, Isoflavone, Flavone, and Flavan-3-ol. ACS Omega 6:8908–8918. https://doi.org/10.1021/acsomega.0c06156

13. Ruiz-Anchondo T, Flores-Holguín N, Glossman-Mitnik D (2010) Natural Carotenoids as Nanomaterial Precursors for Molecular Photovoltaics: A Computational DFT Study. Molecules 15:4490–4510. https://doi.org/10.3390/molecules15074490

14. Ge X, Ding H, Liu T, et al (2025) Visible Light Activation of Anatase TiO2 Achieved by beta-Carotene Sensitization on Earth's Surface. Catalysts 15:739. https://doi.org/10.3390/catal15080739

15. Bouaamlat H, Jabkhiro H, Meneghini C, Tortora L (2026) Effect of donor groups on the photovoltaic performance and TiO2 adsorption of thiophene-based D–π–A dyes for DSSCs: A first-principles study. Mater Chem Phys 348:131616. https://doi.org/10.1016/j.matchemphys.2025.131616

16. Anoua R, Touhtouh S, El Jouad M, et al (2024) Experimental optical properties explained by density functional theory of the natural red algae for dye-sensitized solar cells application. Environ Sci Pollut Res 31:33651–33662. https://doi.org/10.1007/s11356-024-33461-0

17. Calogero G, Marco GD (2008) Red Sicilian orange and purple eggplant fruits as natural sensitizers for dye-sensitized solar cells. Sol Energy Mater Sol Cells 92:1341–1346. https://doi.org/10.1016/j.solmat.2008.05.007

18. Narayan MR (2012) Review: Dye sensitized solar cells based on natural photosensitizers. Renew Sustain Energy Rev 16:208–215. https://doi.org/10.1016/j.rser.2011.07.148

19. M. J. Frisch, G. W. Trucks, H. B. Schlegel, et al (2016) Gaussian 16

20. Becke AD (1993) Density-functional thermochemistry. III. The role of exact exchange. J Chem Phys 98:5648–5652. https://doi.org/10.1063/1.464913

21. Lee C, Yang W, Parr RG (1988) Development of the Colle-Salvetti correlation-energy formula into a functional of the electron density. Phys Rev B 37:785–789. https://doi.org/10.1103/PhysRevB.37.785

22. Hehre WJ, Ditchfield R, Pople JA (1972) Self—Consistent Molecular Orbital Methods. XII. Further Extensions of Gaussian—Type Basis Sets for Use in Molecular Orbital Studies of Organic Molecules. J Chem Phys 56:2257–2261. https://doi.org/10.1063/1.1677527

23. Yanai T, Tew DP, Handy NC (2004) A new hybrid exchange–correlation functional using the Coulomb-attenuating method (CAM-B3LYP). Chem Phys Lett 393:51–57. https://doi.org/10.1016/j.cplett.2004.06.011

24. Preat J, Michaux C, Jacquemin D, Perpète EA (2009) Enhanced Efficiency of Organic Dye-Sensitized Solar Cells: Triphenylamine Derivatives. J Phys Chem C 113:16821–16833. https://doi.org/10.1021/jp904946a

25. Scharber MC, Mühlbacher D, Koppe M, et al (2006) Design Rules for Donors in Bulk-Heterojunction Solar Cells—Towards 10 % Energy-Conversion Efficiency. Adv Mater 18:789–794. https://doi.org/10.1002/adma.200501717

26. Raga SR, Barea EM, Fabregat-Santiago F (2012) Analysis of the Origin of Open Circuit Voltage in Dye Solar Cells. J Phys Chem Lett 3:1629–1634. https://doi.org/10.1021/jz3005464

27. Maragani R, Misra R, Roy MS, et al (2017) (D–π–A)2–π–D–A type ferrocenyl bisthiazole linked triphenylamine based molecular systems for DSSC: synthesis, experimental and theoretical performance studies. Phys Chem Chem Phys 19:8925–8933. https://doi.org/10.1039/c7cp00612h

28. Mandal S, Rao S, Ramanujam K (2017) Understanding the photo-electrochemistry of metal-free di and tri substituted thiophene-based organic dyes in dye-sensitized solar cells using DFT/TD-DFT studies. Ionics 23:3545–3554. https://doi.org/10.1007/s11581-017-2158-y

29. Li M, Kou L, Diao L, et al (2015) Theoretical Study of WS-9-Based Organic Sensitizers for Unusual Vis/NIR Absorption and Highly Efficient Dye-Sensitized Solar Cells. J Phys Chem C 119:9782–9790. https://doi.org/10.1021/acs.jpcc.5b03667

30. Saad Ebied M, Dongol M, Ibrahim M, et al (2022) Effect of carboxylic acid and cyanoacrylic acid as anchoring groups on Coumarin 6 dye for dye-sensitized solar cells: DFT and TD-DFT study. Struct Chem 33:1921–1933. https://doi.org/10.1007/s11224-022-01957-5

31. Pearson RG (1988) Absolute electronegativity and hardness: application to inorganic chemistry. Inorg Chem 27:734–740. https://doi.org/10.1021/ic00277a030

32. Rinky NJ, Islam MM, Hossen J, Islam MA-A-A-A (2023) Comparative study of anti-ulcer drugs with benzimidazole ring as green corrosion inhibitors in acidic solution: Quantum chemical studies. Curr Res Green Sustain Chem 7:100385. https://doi.org/10.1016/j.crgsc.2023.100385

33. Alam MdS, Hossen J, Maruf MdMR, Islam MdA-A-A-A (2026) Computational molecular insights of natural carotenoid photosensitizers for dye-sensitized solar cells: A DFT and TD-DFT study. Mater 13:103329. https://doi.org/10.1016/j.nxmate.2026.103329

34. Diany R, Kerraj S, Atouailaa M, et al (2025) Enhancing the electronic and optical performance of dye-sensitized solar cells with alizarin-based dyes: DFT/TDDFT investigations. Curr Chem Lett 14:597–612

Supplementary Files

This is a list of supplementary files associated with this preprint. Click to download.

- SIfiles.docx